Diffusionlike Motion of the Modulation Wave in Structurally Incommensurate Systems: A NQR Study

G. Papavassiliou, A. Leventis, and F. Milia
National Center for Scientific Research "Demokritos," Ag. Paraskevi, Attiki, 153 10 Athens, Greece

J. Dolinsek
J. Stefan Institute, University of Ljubljana, Jamova 39, SLO-61111 Ljubljana, Slovenia
(Received 26 July 1994)

^{35}Cl NQR measurements of the spin-echo decay in pure Rb_2ZnCl_4 exhibit an exponential t^3 diffusional time dependence, which is the first clear evidence for the existence of slow random-walk-type motion of the incommensurate modulation wave close to the transition temperature T_I. This phenomenon can be described by an effective diffusion constant D_f in a reduced real space, which is settled as the projection of the direct space onto $\frac{1}{4}$ the period length of the modulation wave. The onset of the incommensurate phase is accompanied by nonzero D_f values, which rapidly decrease on going away from T_I.

PACS numbers: 76.60.–k, 64.70.Rh

Incommensurate (I) systems are characterized by the modulation of some local atomic property, which varies in space with a periodicity irrationally related to the periodicity of the host lattice. In structurally I systems the modulation wave (IMW) is formed by the displacements of the ions from their equilibrium positions in the paraelectric unit cell. This frozen-in IMW is not completely static but undergoes thermal fluctuations in phase (phason mode) and amplitude (amplitudon mode).

The existence of a gapless phason (Goldstone) mode is predicted by the continuum model of I phases [1]. This mode represents a slow sliding of the modulation wave with frequencies down to zero. There are, however, no clear experimental evidences for the existence of this mode, as in real structures discrete lattice effects [2,3] and impurities [4] pin the IMW and introduce a finite gap Δ_φ in the phason excitation spectrum. Depinning effects could be induced by thermal fluctuations of the ionic positions or external forces like an electric field in charge density wave systems [5].

Quadrupolar perturbed NMR [6], NQR (nuclear quadrupole resonance) [7], and EPR [8] techniques have been used in the past to study the excitation spectrum of I systems. The phason gap Δ_φ has been experimentally determined in Rb_2ZnCl_4 from spin-lattice relaxation data [6,9] and the estimated value was in the range $10^{10}-10^{12}$ s^{-1} [6,9]. More recent experiments reported a significant influence of thermally induced amplitude and phase fluctuations of the IMW on the spin-lattice relaxation time T_1 and the line shape [10–12] in the vicinity of the paraelectric-incommensurate transition temperature T_I. The spectral windows of the above techniques lie in the kHz–GHz range and they are insensitive to very slow motions with frequencies close to zero.

Here we present the first clear evidence for the existence of random-walk-type slow motions of the IMW in a pure crystal of Rb_2ZnCl_4 by measuring the effective diffusion constant of ^{35}Cl nuclei close to T_I. We demonstrate that ^{35}Cl(1) NQR measurements of the spin-echo decay obey an exponential t^3 time dependence, which can only be attributed to the diffusional random-walk-type slow motions of the IMW in an inhomogeneous electric field gradient (EFG).

In high-field NMR, slow diffusional motions can be detected by measuring the spin-echo decay in a steady [13] or pulsed [14] magnetic field gradient. In zero-field NQR no magnetic field gradients are present. Diffusive effects can, however, be observed in a spatially inhomogeneous EFG, which exists in systems with lattice disorder such as structurally I systems and glasses. What is essential for the observation of random translational motions is the existence of a resonance frequency-space relation. In one-dimensionally modulated Rb_2ZnCl_4, the NQR ^{35}Cl(1) frequency-space relation takes the form [9,15]

$$\omega_0(\mathbf{r}) = \omega_P + \omega_2 \cos^2(\mathbf{q}\cdot\mathbf{r}) . \quad (1)$$

Here ω_P is the paraelectric value of the resonance frequency, $\mathbf{q}$ is the I wave vector, $\omega_2 \propto (T_I - T)^{2\beta}$, and odd powers of $\cos(\mathbf{q}\cdot\mathbf{r})$ are forbidden by the mirror plane symmetry of the high-temperature phase of Rb_2ZnCl_4. This relation is unique, i.e., it represents a one-to-one map between frequency and space only inside one-quarter of the I wavelength. The spatial periodicity of $\omega_0(\mathbf{r})$ allows one to project the direct space onto $\frac{1}{4}$ of a wavelength of the IMW in the direction of the wave propagation. In this way we obtain a reduced real space, which is "folded" in one dimension, and the uniqueness of the relation is recovered. Under the influence of random thermal fluctuations the nuclei make a diffusionlike motion in the folded space. Such a motion can be described by an effective diffusion constant D, which can be measured in an NQR spin-echo decay experiment.

In order to find the spin-echo attenuation in an inhomogeneous EFG, we use the semiclassical description of

NQR [16] with the following Bloch-like equation for the $M_+ = M_x + iM_y$ magnetization in the rotating frame:

$$\frac{\partial M_+}{\partial t} = -i\omega_2 \cos^2(\mathbf{q}\cdot\mathbf{r})M_+ - \frac{M_+}{T_2} + D\nabla^2 M_+ . \quad (2)$$

T_2 is the spin-spin relaxation time and D the diffusion constant. Neglecting small precessional phase shifts arising from diffusion we find the echo amplitude at time $t = 2\tau$:

$$M_+(2\tau) = \sum_{qx'=0}^{2\pi} M_0 \exp(-2\tau/T_2)\exp\left(- D(\omega_2 q)^2 \times \frac{2\tau^3}{3}\sin^2(2qx')\right). \quad (3)$$

Here x' is the direction of the IMW propagation, τ is the separation time between pulses in a two-pulse experiment, and the summation extends over all nuclei on the IMW.

The diffusion damping term in Eq. (3) depends on the position x' of the nucleus on the IMW. Thus it is possible to resolve spectroscopically the diffusion effects at different parts of the IMW by determining the spin-echo decay curves from the Fourier transformed spectra.

Using a new variable $X = \cos^2(qx')$, one obtains the diffusion- and T_2-weighted spectrum at positive frequencies as

$$I^+(\omega) = M_0 e^{-2\tau/T_2}\int_0^1 dX \frac{1}{\sqrt{X(1-X)}}\exp\left(- D(\omega_2 q)^2\frac{2\tau^3}{3}4X(1-X)\right) \times \int_0^\infty \exp[i(\omega-\omega_2 X)t']\exp\left[-\left(\frac{t'}{T_2} + D(\omega_2 q)^2\frac{t'^3}{3}4X(1-X)\right)\right]dt', \quad (4)$$

with $t' = t - 2\tau$. The summation over qx' has been replaced by an integration over X, weighted with the distribution $G(X) = [X(1-X)]^{-1/2}$ [9]. For $T_2 \to \infty$ and $D \to 0$ one obtains from Eq. (4) the static I NQR line shape

$$I(\omega) = \left[\frac{\omega}{\omega_2}\left(1 - \frac{\omega}{\omega_2}\right)\right]^{-1/2}, \quad (5)$$

which exhibits two edge singularities at $\omega = 0$ and $\omega = \omega_2$. The quantity ω_2 can thus be determined experimentally from the splitting of the two edge singularities.

Equation (4) represents a convolution of the static spectrum [Eq. (5)] with the homogeneous line shape, which is a nonanalytical Fourier transform of the expression

$$f(t') = \exp(-t'/T_2)\exp\left(-D(\omega_2 q)^2\frac{t'^3}{3}4X(1-X)\right). \quad (6)$$

Because of the convolution, different parts of the static spectrum are mixed. In that case the homogeneous linewidth is comparable to the width of the static spectrum, the whole spectrum will be attenuated almost uniformly by the diffusion effects. Such a situation is found in the close vicinity of T_I, as the static spectrum width is proportional to $\omega_2 \propto (T_I - T)^{2\beta}$. Far away from T_I the homogeneous linewidth is negligible compared to the static spectrum width and we get the diffusion attenuated spectrum as

$$I(\omega) = \left[\frac{\omega}{\omega_2}\left(1 - \frac{\omega}{\omega_2}\right)\right]^{-1/2}\exp\left(-\frac{2\tau}{T_2}\right)\exp\left[-D(\omega_2 q)^2\left(\frac{2\tau^3}{3}\right)4\left(\frac{\omega}{\omega_2}\right)\left(1 - \frac{\omega}{\omega_2}\right)\right]. \quad (7)$$

Here the attenuation is zero at both edge singularities and maximum in the middle of the spectrum at $\omega = \omega_2/2$.

In our treatment so far we have used the approximation that the effective diffusion of the IMW can be described by a single scalar and constant diffusion coefficient D. We thus do not discriminate between the amplitudon- and the phason-induced diffusive motions. It is known [9,15] that the $\omega = 0$ edge singularity of the NQR spectrum is affected mainly by the phasons, whereas the $\omega = \omega_2$ singularity is affected mainly by the amplitudons. In the middle of the spectrum both effects are mixed. The two types of motion yield different values of the diffusion coefficient D. To remove this deficiency of our description we define a frequency-dependent diffusion constant D_f, which varies over the spectrum and includes the dependence on the X variable—i.e., the different influence of the phason and amplitudon types of motion along the inhomogeneous NQR spectrum. The spectrum amplitude attenuation factor now becomes

$$M(2\tau) = M_0 \exp\left[-\left(\frac{2\tau}{T_2} + D_f(\omega_2 q)^2\frac{2\tau^3}{3}\right)\right]. \quad (8)$$

The diffusion motion has been experimentally observed in nominally pure Rb_2ZnCl_4 on the $^{35}Cl(1)$ line. The NQR line shapes in the vicinity of $T_I = 29$ °C are shown in Fig. 1(a). At T_I, the line starts to broaden, but it remains single peaked for about 1 °C below T_I. There the typical I line shape with two edge singularities starts to appear and transforms into a staticlike line shape about 4 °C below T_I. The region between 29 °C and 28 °C, where the line shape broadens but its shape remains that of the paraphase, corresponds to the case where the homogeneous line shape has larger width than the static I line shape. The splitting between the edge singularities

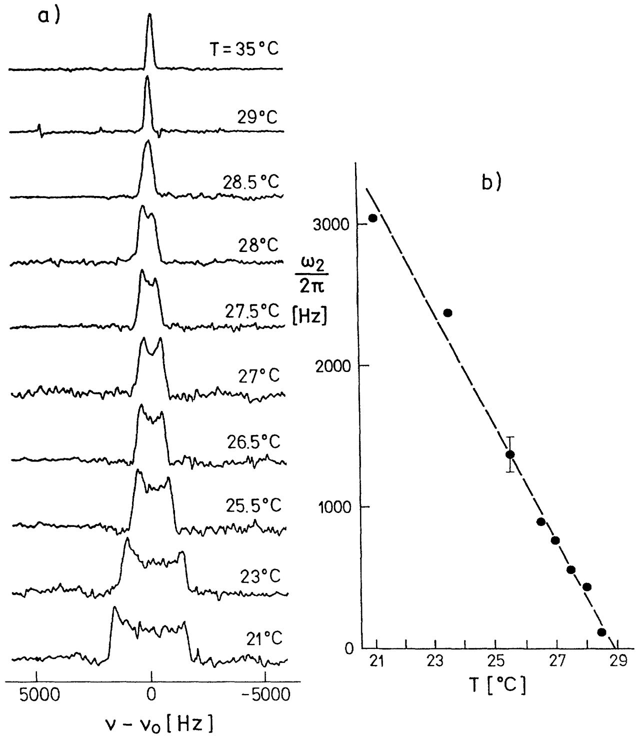

FIG. 1. (a) $^{35}Cl(1)$ NQR line shapes in Rb_2ZnCl_4 in the vicinity of $T_I = 29$ °C. The frequency scales of all spectra are equal, whereas the scale origins are not the same. (b) The splitting of the edge singularities $\omega_2/2\pi$ of the above spectra as a function of temperature.

of the line shapes $\omega_2/2\pi$ of Fig. 1(a) vs temperature is displayed in Fig. 1(b).

Spin-echo decay measurements have been performed in the vicinity of T_I using a pulsed NQR technique. In addition to the decaying behavior of the echo height as a function of the interpulse spacing time τ, slow beats in the echo envelope were found with a frequency of about 2 kHz. These oscillations probably originate from indirect spin-spin interactions [17]. This effect is, however, irrelevant to our problem; it can be accounted for by the fit procedure by using the ansatz

$$M(2\tau) = M_0 \exp\left[-\left(\frac{2\tau}{T_2} + D_f(\omega_2 q)^2 \frac{2\tau^3}{3}\right)\right] \times [1 - C \sin^2(\pi \Delta_i \tau)]. \quad (9)$$

Here C is a constant of the order of 2 [18] and Δ_i is the frequency of the slow beats.

The fit of the echo-decay envelope has been performed on the experimental data obtained from the spectra. At temperatures where the spectra were single peaked, the echo decay envelopes have been determined at the top of the spectra. Below 28 °C two edge singularities have been observed and the envelopes were determined at both singularities and in the middle of the spectrum. The spin-echo decay curves of the paraelectric phase and those obtained on the high frequency singularity of the spectrum as a function of temperature are shown in Fig. 2. It is observed that far above T_I the decay is well described by the T_2 term only. This demonstrates that molecular motions of the diffusive type are not dominant there. T_2 has been determined there to be 780 μs. In the close vicinity of T_I a strong exponential t^3 damping is observed, indicating that the diffusive molecular motion is now dominant. Deep inside the I phase the spin-echo decay is once more described by the T_2 term only, yielding the same value of T_2 as above T_I. The homogeneous linewidth $\Delta\nu_{1/2} = (\pi T_2)^{-1} = 400$ Hz is never negligible to $\omega_2/2\pi$ in the investigated temperature range and Eq. (7) cannot be applied. The diffusional effects are thus properly described by Eq. (4). The same analysis has also been performed on the low frequency singularity and in the middle of the spectrum.

The frequency-dependent diffusion constant D_f as a function of temperature is displayed in Fig. 3. In our determination we used ω_2 values from Fig. 1(b) and the wave vector value close to T_I $q = 2.2 \times 10^7$ cm^{-1} [9]. We further assumed the $T_2 = 780$ μs in the region close to T_I. The results at both edge singularities as well as in the middle of the spectrum are displayed separately. D_f is the largest very close to T_I. At $T = 28.5$ °C, D_f is constant over the whole spectrum and equal to 5.7×10^{-10} cm^2/s. On lowering the temperature the diffusion

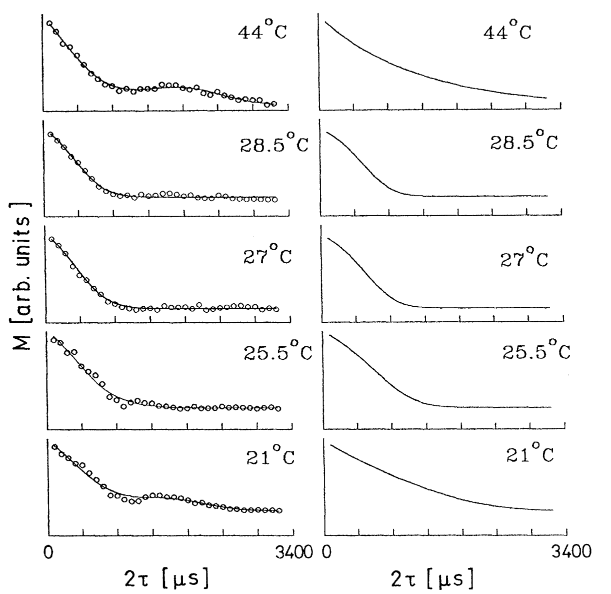

FIG. 2. Temperature dependence of the $^{35}Cl(1)$ spin-echo decay curves in Rb_2ZnCl_4 below and above T_I. Below T_I the curves have been obtained on the high frequency singularity of the NQR spectrum. In the left column experimental points (circles) are shown together with the theoretical curves (solid lines) which have been computed from Eq. (9). The right column shows the theoretical fit curves with the oscillatory part substracted. These curves show the T_2 and diffusive decay only. The exponential decay of the form $\exp[-2\tau/T_2]$ far above and below T_I changes into a diffusive one of the form $\exp[-D_f(\omega_2 q)^2 2\tau^3/3]$ in the vicinity of T_I.

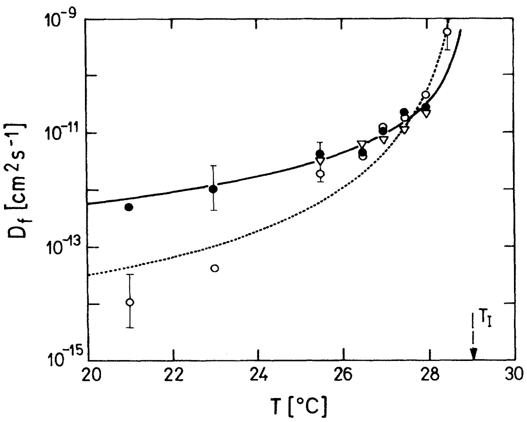

FIG. 3. Temperature dependence of the frequency-dependent diffusion constant D_f close to T_I in Rb_2ZnCl_4. The experimental points show the values of D_f obtained at the high (open circles) and low frequency (solid circles) singularities as well as in the middle (triangles) of the ^{35}Cl(1) NQR spectra. Theoretical curves according to Eq. (10) have been obtained with $\lambda = 3.49$ (dotted curve) and $\lambda = 1.80$ (solid curve).

constant drops continuously from the range 10^{-10} into 10^{-14} cm^2/s and starts to vary over the spectrum below 25.5 °C. What is remarkable are the extremely low D_f values, which are about 6 orders of magnitude smaller than those measured with NMR in a linear magnetic field gradient. This is a consequence of a much larger variation of the frequency with space in the NQR case.

The temperature dependence of the diffusion constant displayed in Fig. 3 can be explained as follows. In the plane-wave approximation and the strong-pinning limit [19], the random-walk-type motion of the IMW can be considered as activated over a barrier $U(A) = 2WA^{\nu}$ [4,20]. Here we made the conjecture that $U(A)$ depends on the νth power of the amplitude $A \propto (T_I - T)^{\beta}$ of the IMW, and W is a coupling constant characterizing the impurity pinning strength. Such motion is described by a diffusion constant $D = \ell^2/\tau_D$, where ℓ is the elementary step of the random walk and τ_D is the transition time per step, which is taken as thermally activated $\tau_D = \tau_{D_0} \exp[U(A)/kT]$. The elementary step ℓ is connected to the impurity density $n(W)$ as $\ell(W) \propto n(W)^{-1/3}$[4], where it is considered that n depends on the impurity pinning strength W. For simplicity we assume that $n(W)$ can be written in the form $n(W) = bW^{-\gamma}$, and calculate the average diffusion constant as

$$D_{\mathrm{av}} = \int_0^{\infty} n(W) \frac{\ell(W)^2}{\tau_D} dW \propto (T_I - T)^{-\lambda}, \qquad (10)$$

where $\lambda = \nu\beta(1 - \gamma/3)$. The effective diffusion constant D_f follows a similar law. According to Eq. (10) D_f behaves critically around T_I and rapidly decreases on lowering the temperature, as was observed also experimentally. Deep inside the I phase diffusional effects become insignificant.

Theoretical curves in Fig. 3 are calculated according to Eq. (10). On the high frequency edge singularity we obtained the exponent $\lambda = 3.49$, whereas in the middle of the spectrum and the low frequency singularity $\lambda = 1.80$. The different λ values indicate that in a more elaborate model one should discriminate between the phason- and amplitudon-induced diffusive motions.

In conclusion, NQR measurements can be used to determine diffusive motions in spatially disordered systems, where the resonance frequency-space relation can be derived. In the case of I Rb_2ZnCl_4, this technique has demonstrated, for the first time, clearly the existence of a slow diffusive motion of the modulation wave in the vicinity of T_I. This was possible because extremely small diffusion constants can be measured with NQR, which are many orders of magnitude smaller than those measured with NMR.

This work has been partially supported by a NATO fund.

[1] A. D. Bruce and R. A. Cowley, J. Phys. C **11**, 3609 (1978).
[2] A. D. Bruce, J. Phys. (Paris) **44**, 147 (1983).
[3] G. Papavassiliou, F. Milia, R. Blinc, and S. Kotsios, Phys. Rev. B **44**, 7283 (1991).
[4] P. Prelovsek, Phase Trans. **11**, 203 (1988).
[5] P. Segransan, A. Jannossy, C. Berthier, J. Marais, and P. Butanol, Phys. Rev. Lett. **56**, 1854 (1986).
[6] B. Topic and U. Haeberlen, Phys. Rev. B **40**, 799 (1989).
[7] F. Milia and G. Papavassiliou, Phys. Rev. B **39**, 4467 (1989).
[8] A. Kaziba and J. C. Fayet, J. Phys. **47**, 239 (1986).
[9] R. Blinc, P. Prelovsek, V. Rutar, J. Seliger, and S. Zumer, in *Incommensurate Phases in Dielectrics,* edited by R. Blinc and A. P. Levanyuk (North-Holland, Amsterdam, 1986), Vol. 1; R. Blinc, Phys. Rep. **79**, 331 (1981); R. Blinc, Phys. Rep. **11**, 3609 (1978).
[10] G. Papavassiliou, A. Anagnostopoulos, and F. Milia, J. Phys. C **5**, 1 (1993).
[11] A. M. Fajdiga, T. Apih, J. Dolinsek, R. Blinc, A. P. Levanyuk, S. A. Minyukov, and D. C. Ailion, Phys. Rev. Lett. **69**, 2721 (1992).
[12] B. Topic, U. Haeberlen, R. Blinc, and S. Zumer, Phys. Rev. B **43**, 91 (1991).
[13] E. L. Hahn, Phys. Rev. **80**, 580 (1950).
[14] E. O. Stejskal and J. E. Tanner, J. Chem. Phys. **42**, 288 (1965).
[15] G. Papavassiliou, F. Milia, R. Blinc, and S. Zumer, Solid State Commun. **77**, 891 (1991).
[16] M. Bloom, E. L. Hahn, and B. Herzog, Phys. Rev. **97**, 1699 (1955).
[17] N. E. Ainbinder and J. G. Shaposhnikov, in *Advances in Nuclear Quadrupole Resonance* (Heyden, London, 1978), Vol. 3, p. 67.
[18] V. S. Geshishkin, N. E. Ainbinder, S. I. Gushchkin, and V. A. Shishkin, Sov. Phys. JETP **28**, 407 (1968).
[19] R. Blinc, J. Dolinsek, P. Prelovsek, and K. Hamano, Phys. Rev. Lett. **56**, 2387 (1986).
[20] R. Blinc, D. C. Ailion, J. Dolinsek, and S. Zumer, Phys. Rev. Lett. **54**, 79 (1985).